

Theoretical analysis on GaAs sub-cell doping concentration for triple-junction solar cells irradiated by proton based on TCAD simulation*

LI Junwei^{1,2}, JIA Weimin², SHI Chengying², WANG Zujun³, and LI Zhengcao^{1**}

1. Key Lab of Advanced Materials (MOE), School of Materials Science and Engineering, Tsinghua University, Beijing 100084, China

2. Xi'an Research Institute of High-Technology, Xi'an 710025, China

3. Northwest Institute of Nuclear Technology, Xi'an 710024, China

(Received 14 June 2022; Revised 6 July 2022)

©Tianjin University of Technology 2022

The degradation on the GaInP/GaAs/Ge triple-junction solar cells was irradiated by proton, and the solar cells with various GaAs sub-cell doping concentrations are modeled by the technology computer aided design (TCAD) simulation. The degradation results of related electrical parameters and external quantum efficiency (*EQE*) are studied. The degradation mechanism irradiated by proton is discussed. The short-circuit current, maximum power and conversion efficiency decrease with the increasing of GaAs sub-cell doping concentration. When the base doping concentration of GaAs sub-cell is $1 \times 10^{16} \text{ cm}^{-3}$, the degradation of short-circuit current is less than that of other base doping concentrations. Furthermore, under proton irradiation, with the increase of doping concentration of GaAs sub-cell, the open-circuit voltage first increases and then decreases. Meanwhile, when the base doping concentration of GaAs sub-cell is $2 \times 10^{17} \text{ cm}^{-3}$, the degradation of open-circuit voltage is less than that of other base doping concentrations. The research will provide the basic theories and device simulation method for GaInP/GaAs/Ge triple-junction solar cells radiation damage evaluation study and radiation hardening, and can provide guidance for the production of triple-junction solar cells in orbit.

Document code: A **Article ID:** 1673-1905(2022)12-0723-7

DOI <https://doi.org/10.1007/s11801-022-2100-z>

GaInP/GaAs/Ge triple-junction solar cells have become the major solar cells for spacecraft power source^[1-4]. Compared with single-junction GaAs solar cell, the GaInP/GaAs/Ge triple-junction solar cells made of three materials with different band gap widths can use a wider range of the solar spectrum. It will increase the utilization of the solar spectrum^[5,6]. However, solar cells are radiated by particles including protons and electrons in the space environment, resulting in performance degradation and even functional failure^[7-10].

A certain amount of research has been carried out to elucidate the degradation of triple-junction solar cells under proton irradiation in space. Through experimental methods, the degradation of related parameter caused by proton irradiation with different energy and fluence is mainly studied^[10,11]. ZHAO et al^[10] studied the degradation characteristics of electron and proton irradiated InGaAsP/InGaAs dual-junction solar cell. The results show that the main electrical parameters and external quantum efficiency (*EQE*) values of solar cell are degraded seri-

ously by irradiation. The degradations of electronic parameters are more serious in proton irradiation compared to electron irradiation when the displacement damage dose is the same. Because the current mismatch between sub-cells, it is different to increase the conversion efficiency further. Recently, researchers presented a metamorphic (MM) growth technique. The epitaxial growth by inverting growth direction is carried out and uses $\text{In}_{1-x}\text{Ga}_x\text{As}$ instead of Ge. LI et al^[2] studied 1 MeV electron and 10 MeV proton irradiation effects on inverted metamorphic (IMM) GaInP/GaAs/InGaAs triple junction solar cell. IMM solar cells exhibited great radiation resistance up on $3.16 \times 10^{10} \text{ MeV/g}$ displacement damage dose electron and proton irradiation level.

Accelerator experiment is the most important method to investigate the parameters degradation induced by particles. However, there is a limitation on experimental method. For instance, experiment limits the analysis the internal parameters degradation of solar cells in particle irradiation process, and it limits the analysis of mechanism.

* This work has been supported by the National Natural Science Foundation of China (Nos.11975135 and 12005017), and the National Basic Research Program of China (No.2020YEB1901800).

** E-mail: zcli@tsinghua.edu.cn

Meanwhile, the experiment can only explore the degradation on solar cells in special energy and fluence, it cannot analysis degradation results of triple-junction solar cells under full energy spectrum. The technology computer aided design (TCAD) is an auxiliary method of experimental research by establishing the model and theoretical calculation, which is used to analyze the degradation caused by particle irradiation^[6-8]. It has many advantages, such as a large amount of data, short time consuming and operability^[12,13]. Most importantly, it has the advantage of adjusting the structure parameters of triple-junction solar cells conveniently and analyzing the difference in degradation performance induced by the same irradiation condition^[13]. More studies about the degradation of solar cells have been studied by using TCAD simulation. The degradations of Si, InP and GaAs single-junction solar cell with different structures and doping concentrations were studied in numerical simulation. The related parameters degradations show the difference in various doping concentrations at the same irradiation condition. LI et al^[4] investigated the degradation on triple-junction solar cells induced by proton and electron irradiation using TCAD simulation. It shows that a threshold value exists in irradiation fluence. When the irradiation fluence is more than this value, the degradation of normalized parameter is proportional to the logarithm of the change of electron fluence. However, in this simulation, the triple-junction solar cells model is established for a specific structure. The effect of different GaAs sub-cell doping concentrations is not very clear under proton irradiation. Therefore, in order to investigate deeply and strength the radiation resistance performance of solar cells in space environments, it is necessary to study the degradation on different GaAs sub-cell doping concentrations induced by space proton irradiation. The TCAD simulation has the advantage of adjusting the structure parameters of triple-junction solar cells conveniently and analyzing the difference in degradation performance induced by the same irradiation condition.

In this paper, the proton radiation effects of GaInP/GaAs/Ge triple-junction solar cells with different doping concentrations on GaAs sub-cell are studied by TCAD simulation. The electrical parameters and *EQE* of triple-junction solar cells with different doping concentrations before and after proton irradiation are measured. The degradation mechanisms of relevant parameter are analyzed.

The modeling and simulation process of typical GaInP/GaAs/Ge triple-junction solar cells irradiated by proton includes modeling, simulation, and theoretical calculation.

The triple-junction solar cells model simulated in this work is referred to as existing research results^[14]. The modeling of GaInP/GaAs/Ge triple-junction solar cells structure is shown in Fig.1. It consists of GaInP top cell, GaAs middle and Ge bottom cell. The GaAs cell and Ge

cell is connected by highly doped tunneling junctions (p⁺-GaAs/n⁺-GaAs). The tunnel junction is defined as a conductor in the vacuum in simulation^[15]. The GaAs sub-cell emitter doping concentration varies from 6×10¹⁷ cm⁻³ to 3×10¹⁸ cm⁻³, and the base doping concentration varies from 1×10¹⁶ cm⁻³ to 3×10¹⁷ cm⁻³. There is no antireflection structure in the simulation and the front surface reflectivity to light is 20%. The AM0 standard spectrum model (*H*₀=1 367 W/m²) as the optical source is used in the triple-junction solar cells model.

After proton irradiation, it interacts with the complex formed by lattice atoms and a large number of vacancies, impurities and gap atoms that lead to traps within the band gaps in triple-junction solar cells. The electron and hole traps irradiated by proton irradiated are acting as the indirect recombination center^[13]. The results show that the trap is the main reason for the degradation after proton irradiation. Therefore, after the proton irradiation experiment, the degradation process of triple-junction solar cells under proton irradiation is simulated by using the electron traps and hole traps measured by deep level transient spectroscopy (DLTS). The number of traps is obtained by multiplying the introduction rate of the traps and proton fluence^[16,17] and Tab.1 shows the defect parameters of GaInP and GaAs obtained by DLTS test after proton irradiation.

			Cathode	
N-Al _{0.25} In _{0.5} Ga _{0.25} P	Window	0.03 μm		
N-In _{0.5} Ga _{0.5} P	Emitter	0.1 μm		Top cell
P-In _{0.5} Ga _{0.5} P	Base	0.58 μm		GaInP
P-In _{0.5} Ga _{0.5} P	BSF	0.03 μm		<i>E_g</i> >1.85 eV
P-GaAs	TJ	0.03 μm		Tunneling
N-GaAs	TJ	0.03 μm		junction
N-In _{0.5} Ga _{0.5} P	Window	0.03 μm		
N-GaAs	Emitter	0.1 μm		Middle cell
P-GaAs	Base	2.5 μm		GaAs
P-In _{0.5} Ga _{0.5} P	BSF	0.03 μm		1.85 eV > <i>E_g</i> > 1.43 eV
P-GaAs	TJ	0.03 μm		Tunneling
N-GaAs	TJ	0.03 μm		junction
N-In _{0.5} Ga _{0.5} P	Window	0.01 μm		
N-Ge	Emitter	0.05 μm		Bottom cell
P-Ge	Substance	170 μm		Ge
				1.43 eV > <i>E_g</i> > 0.67 eV
			Anode	

Fig.1 Modeling of GaInP/GaAs/Ge triple-junction solar cells structure

Through the analysis of the structure of triple-junction solar cells, the sub cells of triple-junction solar cells are connected in series. The total output current of triple-junction solar cell is the minimum current of sub-cell. After proton irradiation, the current generated by the Ge bottom cell is much larger than that of the two others^[9], the Ge sub-cell current does not affect the output current of the triple-junction solar cells. Therefore, the degeneration of

Ge sub-cell is not studied irradiated by proton irradiation. To solve the related parameters of triple-junction solar cells, theoretical calculation contains Poisson's equation and carrier continuity equations are given as^[18]

$$\text{div}(\epsilon \nabla \psi) = -\rho, \quad (1)$$

$$\frac{\partial n}{\partial t} = \frac{1}{q} \text{div} \mathbf{J}_n + G_n - R_n, \quad (2)$$

$$\frac{\partial p}{\partial t} = -\frac{1}{q} \text{div} \mathbf{J}_p + G_p - R_p, \quad (3)$$

$$\mathbf{J}_n = -q \mu_n n \nabla E_n, \quad (4)$$

$$\mathbf{J}_p = -q \mu_p p \nabla E_p, \quad (5)$$

where Eq.(1) is the Poisson's equation, ψ is the electrostatic potential, ϵ is the local permittivity and ρ is the local space charge density. Eqs.(2) and (3) are carrier continuity equations, where R_p and R_n are the hole and electron recombination rates, \mathbf{J}_p and \mathbf{J}_n are the current densities of hole and electron, and q is the magnitude of the charge on an electron. Eqs.(4) and (5) are drift-diffusion transport equations, where μ_p and μ_n are the mobility of hole and electron, and E_p and E_n are the quasi-Fermi levels. In order to simulate the non-radiation of traps irradiated by protons, indirect recombination is introduced into the simulation. The indirect recombination can be expressed as^[12]

$$R_{\text{SRH}} = \sum_{\alpha=1}^m R_{A_\alpha} + \sum_{\beta=1}^n R_{D_\beta}, \quad (6)$$

where R_A is acceptor-like traps recombination rate, R_D is donor-like traps recombination rate, and m and n are the numbers of acceptor-like traps and donor-like traps, respectively. R_A and R_D can be expressed as^[12]

$$R_A = \frac{pn - n_i^2}{\tau_p \left[n + gn_i \exp\left(\frac{E_t - E_i}{kT}\right) \right] + \tau_n \left[p + \frac{1}{g} n_i \exp\left(\frac{E_t - E_i}{kT}\right) \right]}, \quad (7)$$

$$R_D = \frac{pn - n_i^2}{\tau_p \left[n + \frac{1}{g} n_i \exp\left(\frac{E_t - E_i}{kT}\right) \right] + \tau_n \left[p + gn_i \exp\left(\frac{E_t - E_i}{kT}\right) \right]}, \quad (8)$$

where n_i is the intrinsic carrier concentration, E_i and E_t are the intrinsic carrier Fermi level and the defect energy level, T is the absolute Kelvin temperature, g is the degradation factor, and k is the Boltzmann constant.

Tab.1 Defect parameters of GaInP and GaAs obtained by DLTS test after proton irradiation

GaInP		GaAs	
Deep level	E (eV)	Deep level	E (eV)
H1	$E_v+0.20$	H1	$E_v+0.18$
H2	$E_v+0.50$	H2	$E_v+0.23$
H3	$E_v+0.71$	H3	$E_v+0.27$
E1	$E_c-0.20$	H4	$E_v+0.77$
E2	$E_c-0.36$	E1	$E_c-0.14$
E3	$E_c-0.72$	E2	$E_c-0.25$
		E3	$E_c-0.54$
		E4	$E_c-0.72$

Fig.2 shows the change of short-circuit current density (J_{sc}) of simulated triple-junction solar cells with different doping concentrations of GaAs sub-cell emitter under different proton fluences. Fig.3 shows the change of J_{sc} of simulated triple-junction solar cells with different doping concentrations of GaAs sub-cell base under different proton fluences. From Fig.2, one can see that the J_{sc} with different emitter doping concentrations has little difference before proton irradiation. The J_{sc} gradually decreases with increasing of proton fluence under proton irradiation. However, the degeneration of J_{sc} with different emitters and base doping concentrations is different after the same proton fluence, especially when the proton fluence is more than $1 \times 10^{13} \text{ cm}^{-2}$. However, there are some differences between Fig.2 and Fig.3. From Fig.3, the J_{sc} at lower doping concentration is greater than the J_{sc} at higher doping concentration significantly before and after proton irradiation. The J_{sc} in proportion to minority carrier diffusion length (L), and can be expressed as

$$J_{sc} \propto L. \quad (9)$$

Minority carrier diffusion length can be expressed as^[13,19,20]

$$L = \sqrt{D\tau}, \quad (10)$$

$$D = \frac{KT}{q} \mu, \quad (11)$$

$$\mu_n = 9400 / [1 + (N_A / 10^{17})^{0.5}], \quad (12)$$

$$\mu_p = 1 / (0.0025 + 4 \times 10^{-21} N_D), \quad (13)$$

where τ and D are the minority carrier diffusion lifetime and coefficient, μ_n is the electron mobility in GaAs sub-cell p-type base region, and μ_p is the hole mobility in GaAs sub-cell n-type emitter region. N_A and N_D are the acceptor and donor concentrations.

In Eqs.(12) and (13), μ_n and μ_p decrease with the increase of doping concentration. It causes minority carrier diffusion coefficient decreasing and leads to minority carrier diffusion length degeneration with the increase of doping concentration. J_{sc} is mainly made up of base region electron current and emitter region hole current. Because the thickness of GaAs base region is greater than that of emission region, the number of minority carriers in the base region is greater than that of emitter region. It leads to the base region current occupies a large proportion of J_{sc} . Compared with the increasing emitter region doping concentration, more serious degradation on J_{sc} is caused by the increase of GaAs sub-cell base region doping concentration. The minority carrier diffusion length as a function of proton fluence can be expressed as^[18]

$$\frac{1}{L^2} = \frac{1}{L_0^2} + K_L \Phi, \quad (14)$$

where L_0 is the minority carrier diffusion length before proton irradiation, and K_L is the damage coefficient of the minority carrier diffusion length, and Φ is proton

fluence. K_L value is relevant to material properties, doping concentration and proton energy. K_L value increases with the increase of doping concentration. After proton irradiation, the traps introduced by proton irradiation would increase the probability of non-radiative recombination and result in the degeneration of minority carrier lifetime and diffusion length. It will lead to the reduction of the number of minority carriers, which diffuse to the space charge region and produce output current. Therefore, the minority carrier diffusion length decreases with the increase of proton fluence. With the increasing of the emitter and base doping concentration, L_0 gradually decreases, and K_L gradually increases. Both would induce the severe degeneration of J_{sc} .

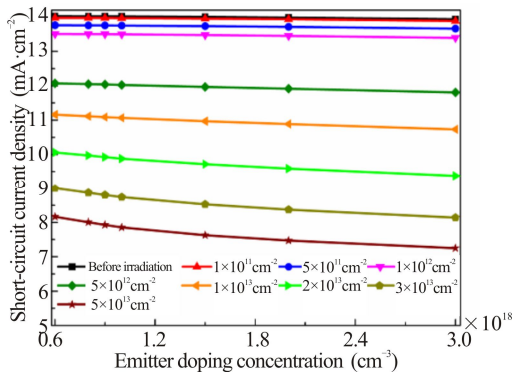


Fig.2 Simulated short-circuit current density versus emitter doping concentration before and after proton irradiation

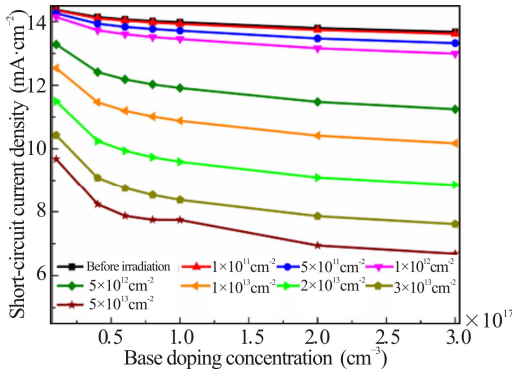


Fig.3 Simulated short-circuit current density versus base doping concentration before and after proton irradiation

Fig.4 shows the change of short-circuit current density (V_{oc}) of simulated triple-junction solar cells with different doping concentrations of GaAs sub-cell emitter under different proton fluences, and Fig.5 shows the change of (V_{oc}) of simulated triple-junction solar cells with different doping concentrations of GaAs sub-cell base under different proton fluences. In Fig.4 and Fig.5, with the increasing of proton fluence, one can see that the V_{oc} gradually decreases. Assuming that all impurities are ionized where $N_A \approx p_p$, $N_D \approx n_n$, and the V_{oc} of each sub-cell can be expressed as^[21]

$$V_{oc_sub-cell} = \frac{kT}{q} \ln \frac{n_n p_p}{n_i^2}, \quad (15)$$

where n_n is majority carrier (electron) concentration in the n-type emitter and p_p is majority carrier (hole) concentration in the p-type base. n_i is intrinsic carrier concentration. As shown in Eq.(15), the V_{oc} increases with the increasing of doping concentration, leading to the V_{oc} of triple-junction solar cells increasing. However, proton radiation will result in the removal of majority carrier, the majority carrier concentration as a function of proton fluence can be expressed as^[21]

$$n = n_0 \exp\left(\frac{-R_c \Phi}{n_0}\right), \quad (16)$$

where n_0 and n are majority carrier concentrations before and after proton irradiation, and R_c is the removal rate of majority carrier concentration. The degradation of majority carrier concentration increases as proton fluence increases, and this will decrease the V_{oc} of triple-junction solar cells. Meanwhile, R_c value increases with the increase of doping concentration, and the R_c increases seriously with the proton fluence increasing. When the fluence is higher, by Eq.(16), this will even lead to the remaining majority carrier with high concentration less than the remaining majority carriers with small concentration after proton irradiation. It results in the open-circuit voltage with high doping concentration is less than the open-circuit voltage with small doping concentration after proton irradiation. Therefore, they will lead to the open-circuit voltage increases firstly and then decreases lightly, as shown in Fig.4 and Fig.5. The V_{oc} of triple-junction solar cells is the sum of the open-circuit voltage of each sub-cell together. The V_{oc} as a function of J_{sc} can be expressed as^[12]

$$V_{oc} = \frac{kT}{q} \sum_{i=1}^3 \ln \left(\frac{J_{sc,i}}{J_{0,i}} + 1 \right), \quad (17)$$

where $J_{sc,i}$ is short-circuit current density of sub-cell, and $J_{0,i}$ is the reverse saturated current density of sub-cell. The relation between the V_{oc} and J_{sc} is approximately logarithm. It results in that the degradation of V_{oc} is less than that of J_{sc} under the same proton irradiation. Before and after proton irradiation, because the change of GaAs sub-cell emitter doping concentration has little effect on the performance of related parameters, the effect of different GaAs sub-cell base doping concentration on related parameters are analyzed under proton irradiation in the following content.

Maximum power is the important parameter that reflects the output performance of triple-junction solar cells. Fig.6 shows the normalized maximum power of triple-junction solar cells with various GaAs base doping concentrations versus proton fluence before and after proton irradiation. From Fig.6, one can see that the normalized maximum power decreases with the increase of proton irradiation. The fluence leads to serious degradation of maximum power that the proton fluence is more

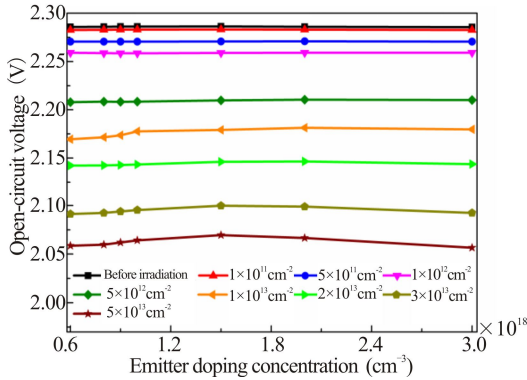


Fig.4 Simulated open-circuit voltage versus emitter doping concentration before and after proton irradiation

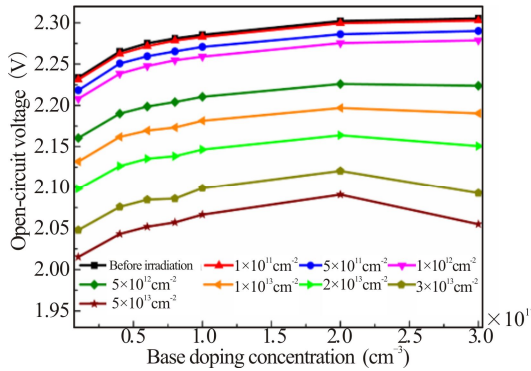


Fig.5 Simulated open-circuit voltage versus base doping concentration before and after proton irradiation

than $1 \times 10^{12} \text{ cm}^{-2}$. The normalized maximum power is as a function of proton fluence, and can be expressed as^[22]

$$\frac{P_{\max}}{P_{\max 0}} = 1 - C \log\left(1 + \frac{\Phi}{\Phi_0}\right), \quad (18)$$

where $P_{\max 0}$ and P_{\max} are the maximum power before and after proton irradiation, and C and Φ_0 are constant. Φ_0 is proton fluence, where the normalized maximum power is a linear function of the logarithm of proton fluence. For triple-junction solar cells with various GaAs sub-cell base doping concentrations, the remaining normalized maximum power is different under the same proton irradiation. Tab.2 is the fitting value of normalized maximum power with various GaAs base doping concentrations by Eq.(18). In Tab.2, the normalized P_{\max} with different base doping concentrations versus proton fluence, and the simulation results have the goodness of fitting with Eq.(18) well. In the meanwhile, Φ_0 decreases as the increasing of base doping concentration. This shows that the threshold fluence, which causes serious degradation of the normalized P_{\max} versus proton fluence, decreases as the increase of base doping concentration.

Conversion efficiency directly reflects the triple-junction solar cells performance, indicating the solar cells utilization of spectrum. Conversion efficiency can be expressed as

$$E_{\text{ff}} = \frac{P_{\max}}{(\text{Optical intensity}) \times A} \times 100\%, \quad (19)$$

where optical intensity is 1367 W/m^2 and A is the solar cell area. Fig.7 shows the simulated conversion efficiency versus GaAs sub-cell base doping concentration. From Fig.7, with the increasing of proton fluence, one can see that the conversion efficiency decreases as the GaAs sub-cell base doping concentration increases. Although the voltage increases with the increasing of base doping concentration, the decrease of current are more serious after the same proton fluence, which results in the E_{ff} decreases as the increasing of GaAs sub-cell base doping concentration.

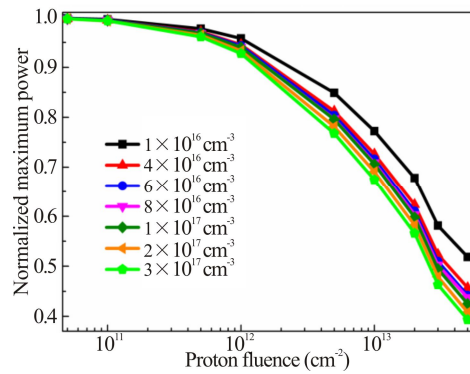


Fig.6 Simulated normalized maximum power with different GaAs sub-cell base doping concentrations versus proton fluence before and after proton irradiation

Tab.2 Fitting values for normalized maximum power with various GaAs sub-cell base doping concentrations by Eq.(18)

GaAs base doping concentration (cm^{-3})	C	Φ_0 (cm^{-2})	R^2
1×10^{16}	0.192	4.290×10^{12}	0.997
4×10^{16}	0.195	3.169×10^{12}	0.998
6×10^{16}	0.197	3.013×10^{12}	0.998
8×10^{16}	0.201	2.929×10^{12}	0.998
1×10^{17}	0.193	2.767×10^{12}	0.998
2×10^{17}	0.198	2.560×10^{12}	0.998
3×10^{17}	0.195	2.257×10^{12}	0.999

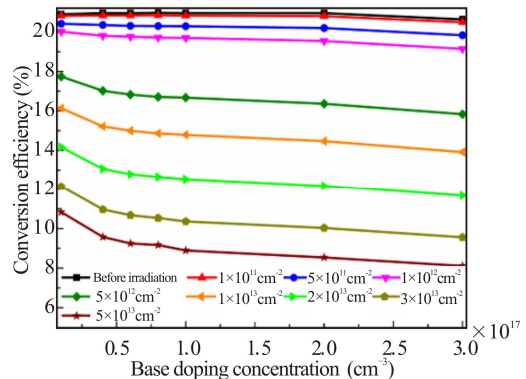


Fig.7 Simulated conversion efficiency versus base doping concentration before and after proton irradiation

The *EQE* is the probability that the incident photon of each wavelength can provide an electron-hole pair to the output circuit. *EQE* can be expressed as

$$EQE(\lambda) = \frac{J_{sc}(\lambda)}{qAQ(\lambda)}, \quad (20)$$

where $Q(\lambda)$ is photon spectrum density. The *EQE* of GaInP/GaAs sub-cells versus different GaAs base doping concentrations before and under proton irradiation for the fluence at $5 \times 10^{13} \text{ cm}^{-2}$ is shown in Fig.8. The degeneration of GaAs middle cell *EQE* is larger than that of GaInP top cell, which shows that the GaAs middle cell radiation resistance is less than that of the GaInP top cell. For *EQE* of GaAs middle cell with various base doping concentrations, the *EQE* with different base doping concentrations has almost no difference before proton irradiation. The *EQE* degeneration of GaAs middle cell increases with the increase of base doping concentration after proton irradiation. It shows that reducing the GaAs middle cell base doping concentration can reduce the *EQE* degradation which is exposed to proton irradiation.

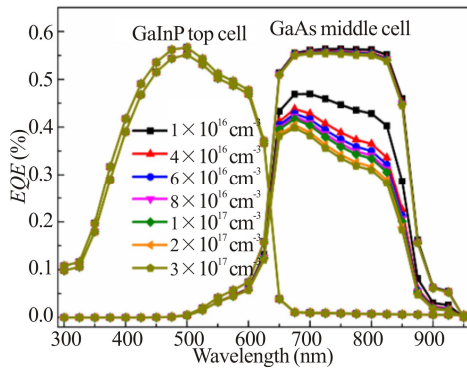


Fig.8 *EQE* of GaInP/GaAs sub-cell with different GaAs sub-cell base doping concentrations before and after proton irradiation at the fluence of $5 \times 10^{13} \text{ cm}^{-2}$

Combined with the analysis above, the short-circuit current density is mainly composed of minority carriers (electron) current density (J_c) of GaAs sub-cell base region. Fig.9(a) shows the J_c of GaAs base region with the doping concentration of $1 \times 10^{16} \text{ cm}^{-3}$ under proton irradiation. In Fig.9(a), J_c decreases with the increase of the distance from the base region to the depletion region. After proton irradiation, electrons diffusion length decreasing leads to the probability of electrons in base region indirection recombination increases with the distance to the depletion region. To intuitively analyze the difference in J_c of GaAs base region with different doping concentrations, the J_c of GaAs base region after proton irradiation along secant line of AA' is obtained by cutline tool as shown in Fig.9(b). When the base thickness more than $1.2 \mu\text{m}$, the J_c of GaAs approximately approaches 0, and the J_c (more than $1.2 \mu\text{m}$) is not shown in the figure.

In common to J_c with the doping concentration of $1 \times 10^{16} \text{ cm}^{-3}$ versus the distance to depletion region, J_c with different doping concentrations decreases with the

increase of the distance from the base position to the depletion region. However, the degradation of J_c gradually increases with the increasing of base doping concentration. Meanwhile, the base region position corresponding to J_c reduction to 0 decreases as the doping concentration increases. When the distance between the base position and depletion region is more than minority carrier diffusion length, this will lead to little current is generated. The remaining electron diffusion length in GaAs sub-cell base region decreases with the increasing the doping concentration and results in the base region position corresponding to J_c decreases with the increasing the doping concentration.

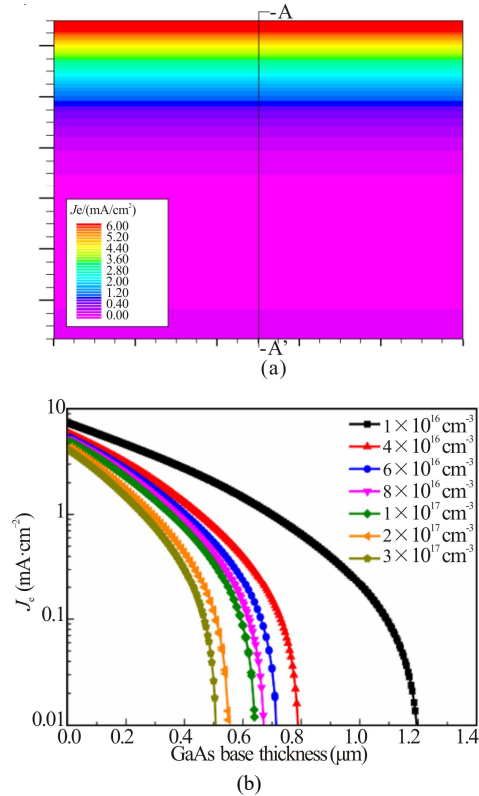


Fig.9 (a) J_c of GaAs sub-cell base region with the doping concentration of $1 \times 10^{16} \text{ cm}^{-3}$ after proton irradiation with fluence at $5 \times 10^{13} \text{ cm}^{-2}$; (b) J_c of GaAs sub-cell base region versus the base doping concentration after proton irradiation with fluence at $5 \times 10^{13} \text{ cm}^{-2}$

In conclusion, the performance of triple-junction solar cells with different doping concentrations of GaAs sub-cell emitter and base under proton irradiation is simulated. The results show that the J_{sc} decreases as the emitter and base doping concentration increasing under the same proton irradiation. The minimum degeneration of short-circuit current occurs when GaAs sub-cell base doping concentration reaches $1 \times 10^{16} \text{ cm}^{-3}$. However, with the increase of GaAs sub-cell emitter and base doping concentration, the V_{oc} firstly increases and then decreases. The minimum degeneration of open-circuit voltage occurs when GaAs sub-cell base doping concentration reaches $2 \times 10^{17} \text{ cm}^{-3}$. The remaining *EQE* of GaAs

sub-cell decreases as base doping concentration increasing after same proton fluence. While the studies overcome the limitations of experimental conditions and explore the effect of doping concentration in different radiation performance. Furthermore, the research would direct the design of triple-junction solar cell, enhancing its performance in irradiation condition.

Statements and Declarations

The authors declare that there are no conflicts of interest related to this article.

References

- [1] KUMAR D, DHEER D K, KUMAR L. Effect of different operating conditions on the conversion efficiency of triple-junction solar cell[J]. *Materials research express*, 2021, 8(3): 035902.
- [2] LI J, AIERKEN A, ZHUANG Y, et al. 1 MeV electron and 10 MeV proton irradiation effects on inverted metamorphic GaInP/GaAs/InGaAs triple junction solar cell[J]. *Solar energy materials and solar cells*, 2021, 224: 111022.
- [3] VASILEION T, LLORENS J M, BUENCUERPO J, et al. Light absorption enhancement and radiation hardening for triple junction solar cell through bioinspired nanostructures[J]. *Bioinspiration & biomimetics*, 2021, 16(5): 056010.
- [4] LI J W, WANG Z J, SHI C Y, et al. Evaluating electron induced degradation of triple-junction solar cell by numerical simulation[J]. *Optoelectronics letters*, 2021, 17(5): 276-282.
- [5] SAEIDNAHAEI S, JO H J, SANG J L, et al. Investigation of the carrier movement through the tunneling junction in the InGaP/GaAs dual junction solar cell using the electrically and optically biased photoreflectance spectroscopy[J]. *Energies*, 2021, 14(638): 1-12.
- [6] HMOUDA R A, MUZYCHKA Y S, DUAN X. Experimental and theoretical modelling of concentrating photovoltaic thermal system with Ge-based multi-junction solar cells[J]. *Energies*, 2022, 15(11): 1-12.
- [7] LI J W, WANG Z J, SHI C Y, et al. Research on the emitter thickness optimization of GaInP/GaAs/Ge triple-junction solar cell under space proton irradiation based on TCAD simulation[J]. *AIP advances*, 2020, 10: 115110.
- [8] KOVAL N E, DA PIEVE F, ARTACHO E. Ab initio electronic stopping power for protons in Ga_{0.5}In_{0.5}P/GaAs/Ge triple-junction solar cells for space applications[J]. *Royal society open science*, 2020, 7(11): 200925-200925.
- [9] WANG R, FENG D, LIU Y H, et al. Effects of 50 keV and 100 keV proton irradiation on GaInP/GaAs/Ge triple-junction solar cells[J]. *Plasma science & technology*, 2012, 14(7): 647-649.
- [10] ZHAO X F, AIERKEN A, HEINI M, et al. Degradation characteristics of electron and proton irradiated InGaAsP/InGaAs dual junction solar cell[J]. *Solar energy materials and solar cells*, 2020, 206: 110339.
- [11] XU Y, HEI M N, SHEN X, et al. Spectral and electrical properties of 3 MeV and 10 MeV proton irradiated InGaAsP single junction solar cell[J]. *Japanese journal of applied physics*, 2019, 58(3): 03.
- [12] ELAHIDOOST A, FATHIPOUR M, MOJAB A. Modelling the effect of 1 MeV electron irradiation on the performance degradation of a single junction Al_xGa_{1-x}As/GaAs solar cell[C]//2012 20th Iranian Conference on Electrical Engineering (ICEE), May 15-17, 2012, Tehran, Iran. New York: IEEE, 2012.
- [13] AUGUSTINE G, ROHATGI A, JOKERST N M. Base doping optimization for radiation-hard Si, GaAs, and InP solar cells[J]. *IEEE transactions on electron devices*, 1992, 39(10): 2395-2400.
- [14] LEEM J W, YU J S, KIM J N, et al. Theoretical modeling and optimization of III-V GaInP/GaAs/Ge monolithic triple-junction solar cell[J]. *Journal of the Korean Physical Society*, 2014, 64(10): 1561-1565.
- [15] DANIEL S. Modeling radiation effects on a triple junction solar cell using silvaco ATLAS[D]. Monterey: Naval Postgraduate School, 2012.
- [16] KHAN A, YAMAGUCHI M, BOURGOIN J, et al. Deep level transient spectroscopy analysis of 10 MeV proton and 1 MeV electron irradiation-induced defects in p-InGaP and InGaP-based solar cell[J]. *Japanese journal of applied physics*, 2014, 41(3a): 1241-1246.
- [17] GONZALEZ M, ANDRE C L, WALTERS R J, et al. Deep level defects in proton radiated GaAs grown on metamorphic SiGe/Si substrates[J]. *Journal of applied physics*, 2006, 100(3): 1055.
- [18] Silvaco International. Atlas user's manual[EB/OL]. (2018-01-01) [2022-04-15]. <http://www.silvaco.com>.
- [19] HU J M, WU Y Y, QIAN Y, et al. Damage of electron irradiation to the GaInP/GaAs/Ge triple-junction solar cell[J]. *Acta physica sinica*, 2009, 58(7): 5051-5056.
- [20] FURUTA T, TANIYAMA H, TOMIZAWA M. Minority electron transport property in p-GaAs under high electric field[J]. *Journal of applied physics*, 1990, 67(1): 293-299.
- [21] LI J W, WANG Z J, SHI C Y, et al. Modeling and simulating of radiation effects on the performance degradation of GaInP/GaAs/Ge triple-junction solar cells induced by different energy protons[J]. *Acta physica sinica*, 2020, 69(9): 098802.
- [22] ANSPAUGH B E. GaAs solar cell radiation handbook[M]. California: Jet Propulsion Laboratory, 1996.